Physiological Proteomics of the Uncultured Endosymbiont of Riftia pachyptila
Stephanie Markert, *et al.*
Science **315**, 247 (2007);
DOI: 10.1126/science.1132913

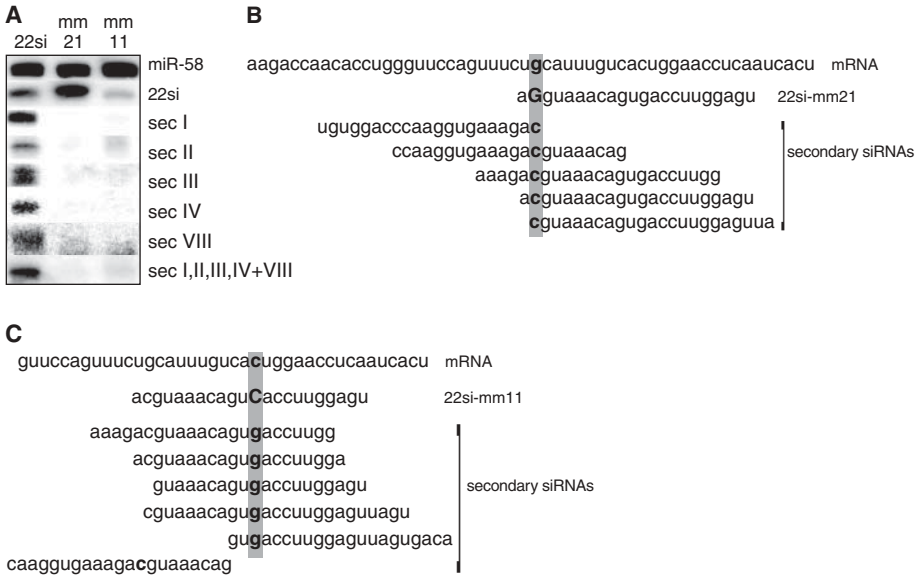

Fig. 3. Secondary siRNAs result from unprimed cRNA synthesis. (**A**) RNA gel blot detection of primary and secondary siRNAs in 22si- and 22si-mm10,11,12 lines. (**B**) Sequence of secondary siRNAs cloned from 22si-mm21 lines. The gray bar indicates mismatch 21. (**C**) Sequence of secondary siRNAs cloned from 22si-mm11 lines. The gray bar indicates mismatch 11.

occurs only unprimed. The 22siRNA is bound by RDE-1 (Fig. 1B and fig. S3A), which carries the DDH motif needed for RISC cleavage (*21*). The presence of a mismatch at the presumed RISC cleavage site in the 22si-mm11 primary siRNA did not alter the range of secondary siRNAs that were cloned (Fig. 3C, table S2), suggesting that nematode RNAi does not primarily depend on RISC cleavage of mRNAs. A minority of the secondary siRNAs is loaded into the RNAi-specific argonaute protein RDE-1 (fig. S3, A and B), and most secondary siRNAs may be loaded into secondary Argonaute proteins (*15*) (fig. S3C). The phased register in which the secondary siRNAs appear to be ordered (Fig. 2A) may arise from multiple amplification rounds (by RDE-1–loaded secondary siRNAs) or from preferred initiation sites of cRNA synthesis.

Secondary siRNAs represent a distinct class of 21- to 22-nt small RNAs that can can silence mRNAs in trans (*3*). They result from unprimed RNA synthesis (Fig. 3, B and C), are only of antisense polarity (Fig. 1A), carry 5′ di- or triphosphates (Fig. 2, C to E), and are mainly loaded into a distinct set of Argonaute proteins (*15*) (fig. S3). Secondary siRNAs can be produced on non–RISC-cleaved mRNAs presumably by internal entry of the RdRP. A 3′ nonprogressive DICER cleavage may be responsible for generating the secondary siRNA 3′ end and degrading the mRNA (fig. S4). We find that for the 22siRNA, a single-nucleotide mismatch decreases silencing efficiency considerably. Likely, these strict prerequisites for inducing transitive RNAi protect organisms against unintended off-target effects (*22*, *23*).

References and Notes

1. G. J. Hannon, *Nature* **418**, 244 (2002).
2. O. Voinnet, P. Vain, S. Angell, D. C. Baulcombe, *Cell* **95**, 177 (1998).
3. T. Sijen *et al.*, *Cell* **107**, 465 (2001).
4. F. E. Vaistij, L. Jones, D. C. Baulcombe, *Plant Cell* **14**, 857 (2002).
5. M. Wassenegger, G. Krezal, *Trends Plant Sci.* **11**, 142 (2006).
6. W. Schiebel, B. Haas, S. Marinkovic, A. Klanner, H. L. Sanger, *J. Biol. Chem.* **268**, 11858 (1993).
7. E. V. Makeyev, D. H. Bamford, *Mol. Cell* **10**, 1417 (2002).
8. B. O. Petersen, M. Albrechtsen, *Plant Mol. Biol.* **58**, 575 (2005).
9. M. Ronemus, M. W. Vaughn, R. A. Martienssen, *Plant Cell* **18**, 1559 (2006).
10. E. A. Parizotto, P. Dunoyer, N. Rahm, C. Himber, O. Voinnet, *Genes Dev.* **18**, 2237 (2004).
11. E. Allen, Z. Xie, A. M. Gustafson, J. C. Carrington, *Cell* **121**, 207 (2005).
12. V. Gasciolli, A. C. Mallory, D. P. Bartel, H. Vaucheret, *Curr. Biol.* **15**, 1494 (2005).
13. M. N. Alder, S. Dames, J. Gaudet, S. E. Mango, *RNA* **9**, 25 (2003).
14. M. Tijsterman, R. F. Ketting, K. L. Okihara, T. Sijen, R. H. Plasterk, *Science* **295**, 694 (2002).
15. E. Yigit *et al.*, *Cell* **127**, 747 (2006).
16. G. Hutvagner, P. D. Zamore, *Science* **297**, 2056 (2002).
17. H. Tabara *et al.*, *Cell* **99**, 123 (1999).
18. H. Tabara, E. Yigit, H. Siomi, C. C. Mello, *Cell* **109**, 861 (2002).
19. A. A. Caudy *et al.*, *Nature* **425**, 411 (2003).
20. V. V. Vagin *et al.*, *Science* **313**, 320 (2006).
21. F. V. Rivas *et al.*, *Nat. Struct. Mol. Biol.* **12**, 340 (2005).
22. Y. Fedorov *et al.*, *RNA* **12**, 1188 (2006).
23. A. L. Jackson *et al.*, *RNA* **12**, 1179 (2006).

24. We thank G. Hannon and F. Rivas for help with the capture assays; R. Ketting for sharing unpublished data on the identity of *mut-15* and for the 5′ linker; M. Verheul, J. van de Belt, and E. Berezikov for help with sequence analyses; C. Mello for providing strains; M. Darding for experimental help; B. Ason and M. Joosten for critically reading the manuscript; and A. Fire for the suggestion to use 9:1 gels. The work was supported by a Vidi fellowship from the Dutch Scientific Organization (NWO) to T.S. and a European Union grant (HPRN-CT-2002-00257) and Netherlands Genomic Initiative grant (050-72-415) to F.A.S.

Supporting Online Material

www.sciencemag.org/cgi/content/full/1136699/DC1
Materials and Methods
Figs. S1 to S4
Tables S1 and S2
References

24 October 2006; accepted 28 November 2006
Published online 7 December 2006;
10.1126/science.1136699
Include this information when citing this paper.

Physiological Proteomics of the Uncultured Endosymbiont of *Riftia pachyptila*

Stephanie Markert,[1] Cordelia Arndt,[2] Horst Felbeck,[3] Dörte Becher,[1] Stefan M. Sievert,[4] Michael Hügler,[4] Dirk Albrecht,[1,5] Julie Robidart,[3] Shellie Bench,[6] Robert A. Feldman,[7] Michael Hecker,[1,5] Thomas Schweder[1,5]*

The bacterial endosymbiont of the deep-sea tube worm *Riftia pachyptila* has never been successfully cultivated outside its host. In the absence of cultivation data, we have taken a proteomic approach based on the metagenome sequence to study the metabolism of this peculiar microorganism in detail. As one result, we found that three major sulfide oxidation proteins constitute ~12% of the total cytosolic proteome, which highlights the essential role of these enzymes for the symbiont's energy metabolism. Unexpectedly, the symbiont uses the reductive tricarboxylic acid cycle in addition to the previously identified Calvin cycle for CO_2 fixation.

Riftia pachyptila inhabits deep-sea hydrothermal vent areas along mid-ocean ridges in the East Pacific (*1*). Instead of containing a digestive system, the worm's coelomic cavity is densely populated by a single species of sulfide-oxidizing gamma-proteobacteria that provide for their host's carbon and energy supply by fixing CO_2 from the surrounding water (*2*–*4*). Microbial chemosynthesis is sustained by the presence of H_2S originating from reduced hydrothermal fluids and oxygen in the seawater (*5*). Compared with free-living sulfur oxidizers, the symbionts benefit from high nutrient concentrations within the worm's body (*6*), which allow for a high metabolic activity. The microbially produced carbon compounds are transferred to the host, making *R. pachyptila* one of the fastest-growing marine invertebrates known (*7*).

We took a functional genomics approach to analyze the proteome and hence to derive

information on the physiology of the uncultured *Riftia* symbionts. The sequencing of the symbiont genome was conducted by a metagenome approach. Bacterial symbionts were isolated and separated from the host tissue, the so-called trophosome (*8*). Using one- and two-dimensional (2D) gel electrophoresis, we established reference maps (master gels) of the soluble intracellular and the membrane-associated bacterial proteome, on which more than 220 identified proteins have been registered so far (Fig. 1 and fig. S1). Our procedures were reproducible and showed the presence of a single endosymbiont species (*9*) with no indication of other bacterial or host tissue contaminants. The proteomic approach provided evidence regarding which of the predicted genes are expressed under natural growth conditions. Levels of protein synthesis reflect the relative proportion of translational capacity that is invested in the individual metabolic paths, and we can deduce the relevance of particular proteins for the symbionts' physiology. On the basis of our proteome data, we were thus able to deduce major pathways of the symbionts' metabolism, e.g., the sulfide oxidation pathway (fig. S2) and the reverse tricarboxylic acid (TCA) cycle (fig. S3), as well as to make inferences about the symbionts' response to oxidative stress.

Although great advances have been made in our understanding of the sulfur oxidation pathways in a variety of sulfur oxidizers in recent years, this pathway remains incompletely characterized in *Riftia* symbionts. In this proteome study, the enzymes DsrA (dissimilatory sulfite reductase), AprA/AprB (adenosine phosphosulfate reductase), and SopT [adenosine triphosphate (ATP) sulfurylase] were identified, which suggested the reactions displayed in fig. S2: H_2S is

[1]Institute of Marine Biotechnology, Walther-Rathenau-Strasse 49, D-17489 Greifswald, Germany. [2]Max-Planck-Institute for Infection Biology, D-10117 Berlin, Germany. [3]Scripps Institution of Oceanography, La Jolla, CA 92093–0202, USA. [4]Woods Hole Oceanographic Institution, Woods Hole, MA 02543, USA. [5]Ernst-Moritz-Arndt-University, D-17487 Greifswald, Germany. [6]University of California Santa Cruz, Santa Cruz, CA 95064, USA. [7]SymBio Corporation, Menlo Park, CA 94025, USA.

*To whom correspondence should be addressed. E-mail: schweder@uni-greifswald.de

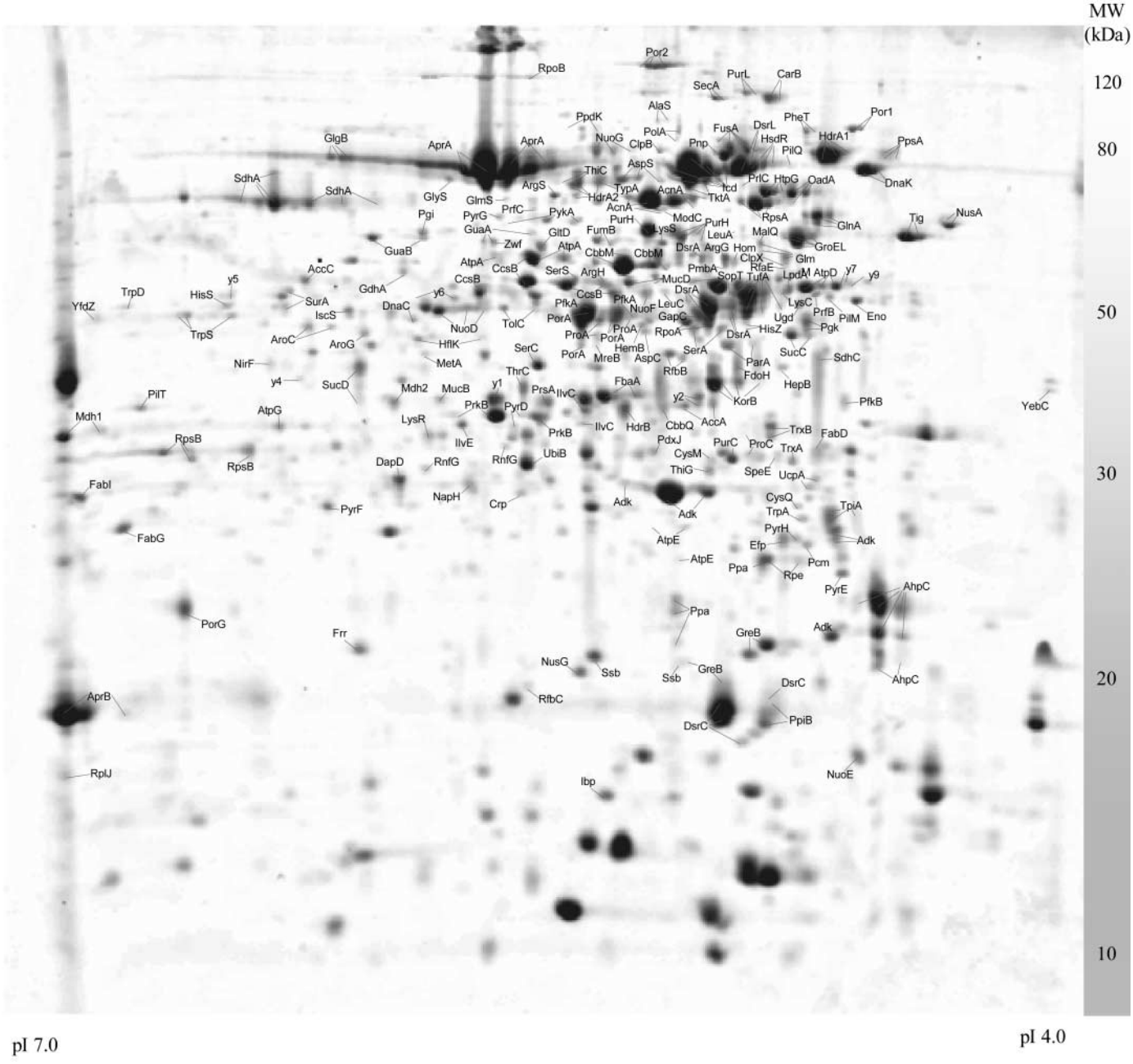

Fig. 1. Reference map of the *Riftia pachyptila* endosymbionts' intracellular proteome. Identified symbiont proteins are indicated. Protein functions are listed in table S1.

oxidized to SO_3^{2-} in a six-electron step; this is subsequently converted to adenosine phosphosulfate (APS), with consumption of adenosine monophosphate (AMP). The final oxidation step yields ATP by substrate-level phosphorylation and simultaneously creates the end product, SO_4^{2-}. Although these enzymes were originally described as part of the reverse pathway in sulfate-reducing bacteria (as reflected in their names), it has long been proposed that they can function just as well in the opposite direction (*10*). Quantitative analyses of the respective protein spots in our study revealed that the three major sulfide oxidation proteins DsrA, AprA/AprB, and SopT constitute more than 12% of the total cytosolic symbiont proteome in a pH range of 4 to 7. This highlights the essential role of these enzymes for the symbiont's energy metabolism.

Table 1. Comparison of *Riftia* symbiont protein spot intensities under high- and low-sulfur conditions. Spot intensities of selected proteins were compared in 2D gel images from sulfur-rich and sulfur-depleted trophosome samples (see SOM for details). Positive ratios represent the factor by which the respective spot intensity was higher on the gels from sulfur-rich trophosomes. Negative ratios give the factor by which spot intensity was higher under low-sulfur conditions. The listed protein spots are highlighted in Fig. 2.

Protein	Function	Spot ratio
	Proteins with higher spot intensity in sulfur-rich trophosome samples	
AprA	Adenylylsulfate reductase, α subunit	8.20
CbbM	RuBisCO form II, large subunit	4.29
DsrA	Dissimilatory sulfite reductase, α subunit	3.55
HdrA2	Heterodisulfide reductase, subunit A	2.26
DsrL	Predicted NADPH:acceptor oxidoreductase	1.92
DsrC	Dissimilatory sulfite reductase, γ subunit	1.47
AprB	Adenylylsulfate reductase, β subunit	1.30
	Proteins with higher spot intensity in sulfur-depleted trophosome samples	
SdhA	Putative fumarate reductase, flavoprotein subunit	−23.83
OadA	Oxaloacetate decarboxylase, α subunit	−15.00
Por1	Pyruvate:flavodoxin/ferredoxin oxidoreductase	−8.58
SucC	Succinyl CoA ligase, β subunit	−6.75
PorG	Pyruvate:ferredoxin/flavodoxin oxidoreductase, γ subunit	−6.13
KorB	2-Oxoglutarate synthase, β subunit	−4.57
AcnA	Aconitase A	−4.50
Mdh1	Malate dehydrogenase	−2.36
SucD	Succinyl-CoA synthetase, α subunit	−2.12
PorA	Pyruvate:flavodoxin/ferredoxin oxidoreductase, α subunit	−2.03

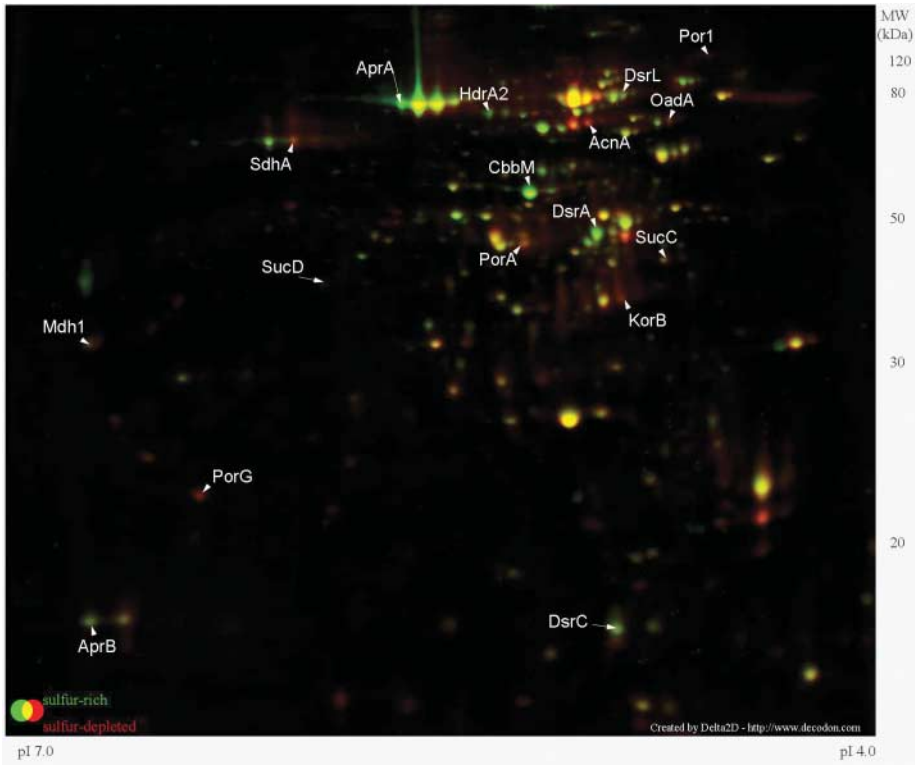

Fig. 2. Comparison of protein patterns under high- and low-sulfur conditions. Images of the 2D gels were colored (sulfur-rich, green, and sulfur-depleted tissue, red spots) and overlaid. Selected proteins with distinct variations in their relative spot volumes from one gel to the other are indicated (see SOM for details).

Using our intracellular protein master gel, we also examined the *Riftia* symbiont's carbon metabolism. We identified most of the enzymes involved in the energy-generating TCA cycle. Moreover, we found the enzyme 2-oxoglutarate: ferredoxin oxidoreductase β subunit (KorB), several copies of a pyruvate:ferredoxin oxidoreductase (subunits Por1, Por2, and PorA/PorG), a putative fumarate reductase (subunits SdhA/SdhC), and a protein highly similar to a citryl–coenzyme A (CoA) synthetase subunit (CcsB). These enzymes could run the TCA cycle in the reductive direction (fig. S3). This cycle represents an alternative CO_2 fixation mechanism that requires less energy than the Calvin cycle for each three-carbon unit formed. Considering the great abundance of these four key enzymes on the protein gels (see relative spot volumes in table S1), we suggest that the reductive TCA cycle is not only a possibility, but a very important feature of the *Riftia* symbiont's carbon metabolism.

To verify the symbiont's capability for using the reductive TCA cycle for CO_2 fixation, we tested cell extracts of isolated bacteria for activity of the above-mentioned key enzymes: The assays clearly revealed specific enzyme activities in all four cases that are higher than those previously reported for ribulose-1,5-bisphosphate carboxylase-oxygenase (RuBisCO) (*11*) (table S2).

The results of our proteome analysis, in combination with the measured enzyme activities, provide strong evidence that the *Riftia* symbionts, which have been considered a prime example for chemolithoautotrophic carbon fixation via the Calvin cycle, use, at least partly, the reductive TCA cycle for autotrophic carbon fixation as well. This might explain the long-standing dilemma that the stable carbon isotopic composition of the *Riftia* symbiont is substantially heavier ($\Delta^{13}C$ of –9 to –16‰) than would be expected by the use of the Calvin cycle alone (*12*). The observed isotopic variation most likely results from varying contributions by the reductive TCA cycle and the Calvin cycle. It is also interesting to note that, concordant with previous findings (*12*), RuBisCO constitutes only ~1% of the *Riftia* symbiont's total protein on our gels. This is a small percentage compared with other bacteria that use only the Calvin cycle for CO_2 fixation, where RuBisCO is usually the major protein and can account for 4 to 50% of the total soluble protein (*13*). The apparent discrepancy between the low concentration and the relatively high activity of RuBisCO in the trophosome (*4*) and the possible occurrence of two carbon fixation pathways in one organism certainly warrant further investigations.

Riftia symbionts can store elemental sulfur in their periplasm if high concentrations of H_2S are available (*14*); these stores result in a light green, almost yellow trophosome. The tissue appears dark green or black (*15*) when sulfur is limiting. To analyze the symbionts' potential responses to changing environmental conditions, we compared bacterial protein patterns from naturally occurring sulfur-rich and from sulfur-depleted trophosome tissues. Under high-sulfide conditions, the resulting 2D gels revealed a distinctly higher spot intensity for enzymes involved in sulfide oxidation and for RuBisCO, compared with low-sulfur conditions (Table 1, Fig. 2). Spot intensities of the sulfide oxidation enzymes AprA and DsrA were about eight and four times, respectively, those under low-sulfur conditions. This indicates that *Riftia* symbionts are capable of adjusting the production of enzymes needed for energy metabolism to the prevailing environmental conditions. In bacteria from tissue with little or no stored sulfur (dark trophosomes), the protein spot volume of the putative fumarate reductase subunit SdhA was about 24 times as high as, and the spot volume of the putative pyruvate:ferredoxin oxidoreductase Por1 was about 9 times as high as that in sulfur-rich, light trophosome (Fig. 2, Table 1). Several other enzymes involved in the reductive TCA cycle, including two other pyruvate:ferredoxin oxidoreductase subunits, PorG and PorA, and the 2-oxoglutarate synthase subunit KorB, could also be detected with elevated spot volumes in samples from sulfur-depleted trophosomes. This suggests that the *Riftia* symbiont might be capable of adapting to a temporary low-energy situation by adjusting its way of carbon fixation: The use of the Calvin cycle might be reduced in favor of the up-regulation of the energetically more favorable reductive TCA cycle. Because *Riftia* symbionts have also been shown to produce glycogen as a carbon storage compound (*16*), it might even be speculated that—for example, under long-lasting or severe low-energy conditions—their metabolism switches from an autotrophic mode to a heterotrophic mode. In this case, the symbiont might revert to burning carbon reserves through glycolysis and the oxidative TCA cycle to generate energy and precursors for biosynthesis. The symbiont might thus be able to use the TCA cycle in the oxidative and reductive direction, depending on the environmental conditions, which would allow for a high metabolic flexibility. Apparently, the true nature of the *Riftia* symbiont's metabolic strategies is much more complex than expected. Further detailed investigations are needed to explicitly evaluate and validate these hypotheses.

Physiological tests revealed that *Riftia* symbionts do not have a catalase to protect the cells from H_2O_2 (*17*). This result is supported by the lack of the respective gene in the metagenome sequence. Because *Riftia* symbionts do not tolerate high oxygen concentrations (*18*), we tested their strategy of coping with stress situations caused by hydrogen peroxide. Our experiments revealed a strong induction of the alkyl hydroperoxide reductase AhpC (Fig. 3). This enzyme is present in large amounts in the cytoplasmic protein fraction (Fig. 1) and reduces organic hydroperoxides caused by H_2O_2. Our results indicate that AhpC plays a crucial role in the resistance of these microaerophilic bacteria to oxidative stress.

This study shows that a comparative proteomic view of the *Riftia* symbionts' cell physiology allows for a complex physiological description without their cultivation. It reaches beyond the mere prediction of putative metabolic functions as coded in the genome sequence.

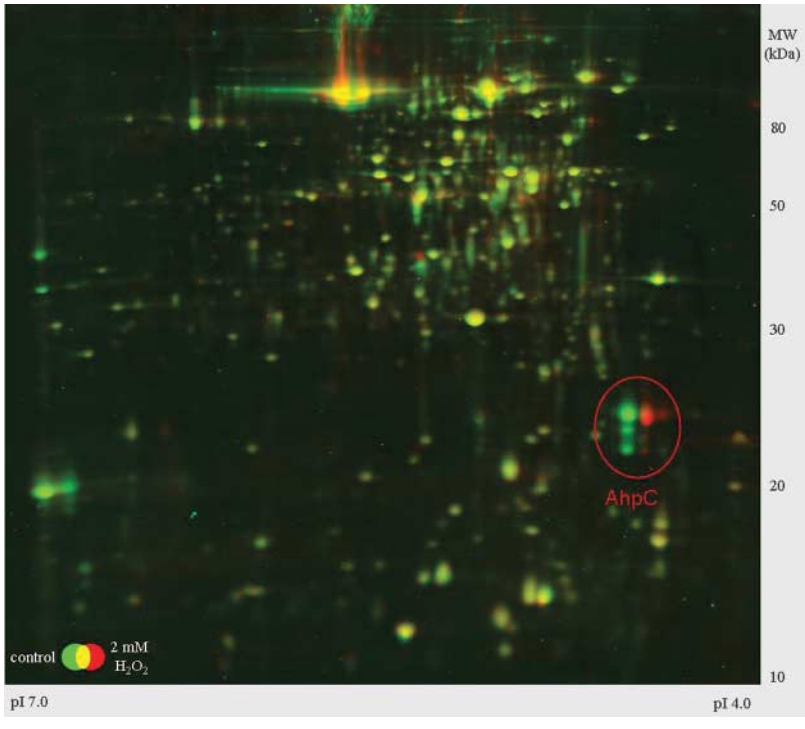

Fig. 3. Comparison of protein patterns in response to oxidative stress. The 2D gels show proteins from samples taken before and 60 min after the addition of 2 mM H_2O_2 to a suspension of isolated *Riftia* symbionts. Both images were colored (control, green spots, and stress sample, red spots) and overlaid. The oxidative stress protein AhpC is indicated. Because of the delayed deformylation of the newly synthesized protein during the massive induction of AhpC production, the protein spot shifts to a slightly more acidic pH. The "new" AhpC, produced after the stress with H_2O_2 is thus visible as red spots right next to the "old" AhpC, visible as green spots.

References and Notes

1. M. L. Jones, *Science* **213**, 333 (1981).
2. C. M. Cavanaugh, S. L. Gardiner, M. L. Jones, H. W. Jannasch, J. B. Waterbury, *Science* **213**, 340 (1981).
3. H. Felbeck, J. J. Childress, *Oceanol. Acta* **8**, 131 (1988).
4. H. Felbeck, J. J. Childress, G. N. Somero, *Nature* **293**, 291 (1981).
5. H. W. Jannasch, M. J. Mottl, *Science* **229**, 717 (1985).
6. J. J. Childress, C. R. Fisher, *Oceanogr. Mar. Biol. Annu. Rev.* **30**, 337 (1992).
7. R. A. Lutz *et al.*, *Nature* **371**, 663 (1994).
8. D. L. Distel, H. Felbeck, *J. Exp. Zool.* **247**, 1 (1988).
9. D. A. Stahl, D. J. Lane, G. J. Olsen, N. R. Pace, *Science* **224**, 409 (1984).
10. M. Schedel, M. Vanselow, H. G. Trüper, *Arch. Microbiol.* **121**, 29 (1979).
11. D. C. Nelson, C. R. Fisher, in *Microbiology of Deep-Sea Hydrothermal Vents*, D. M. Karl, Ed. (CRC Press, Boca Raton, FL, 1995), pp. 125–167.
12. J. J. Robinson *et al.*, *Limnol. Oceanogr.* **48**, 48 (2003).
13. F. R. Tabita, *Microbiol. Rev.* **52**, 155 (1988).
14. D. B. Wilmot, R. D. Vetter, *Mar. Biol.* **106**, 273 (1990).
15. B. Pflugfelder, C. R. Fisher, M. Bright, *Mar. Biol.* **146**, 895 (2005).
16. A. Sorgo, F. Gaill, J. P. Lechaire, C. Arndt, M. Bright, *Mar. Ecol. Prog. Ser.* **231**, 115 (2002).
17. J. Blum, I. Fridovich, *Arch. Biochem. Biophys.* **228**, 617 (1984).
18. C. R. Fisher, J. J. Childress, E. Minnich, *Biol. Bull.* **177**, 372 (1989).

19. We appreciate the great help of M. Bright and thank J. Childress and C. Cary for inviting us on their cruises. Thanks also to A. Dreisbach, U. Völker, J. Bernhardt, M. Kleiner, and M. Fraunholz. This work was supported by the Deutsche Forschungsgemeinschaft, grant Schw595/3-1. Other funding sources were NSF (OCE 04-52333) and U.S. National Aeronautics and Space Administration Astrobiology Institute (NNA04CC04A) for S.M.S., postdoctoral scholarship from Woods Hole Oceanographic Institution to M.H., and Academic Senate of the University of California (RF811S and RE518S) to H.F. The *Riftia* symbiont nucleotide sequence has been deposited as a whole-genome shotgun project at DDBJ/EMBL/GenBank under the project accession AASF00000000. The version referred to in this study is the first version, AASF01000000. For all proteins addressed in this study, the annotation results were submitted to GenBank (see table S1).

Supporting Online Material

www.sciencemag.org/cgi/content/full/315/5809/247/DC1
Materials and Methods
SOM Text
Figs. S1 to S3
Tables S1 and S2
References and Notes

24 July 2006; accepted 14 November 2006
10.1126/science.1132913